

Gamma spectroscopy of environmental samples

P. B. Siegel^{a)}

California State Polytechnic University Pomona, Pomona, California 91768

(Received 19 February 2012; accepted 13 February 2013)

We describe experiments for the undergraduate laboratory that use a high-resolution gamma detector to measure radiation in environmental samples. The experiments are designed to instruct the students in the quantitative analysis of gamma spectra and secular equilibrium. Experiments include the radioactive dating of Brazil nuts, determining radioisotope concentrations in natural samples, and measurement of the ^{235}U abundance in uranium rich rocks. © 2013 American Association of Physics Teachers. [<http://dx.doi.org/10.1119/1.4793595>]

I. INTRODUCTION

Experiments involving nuclear radiation detection are routinely performed in the undergraduate physics curriculum. Common detectors found in many undergraduate institutions are Geiger counters and sodium iodine (NaI) gamma detectors. These detectors are relatively inexpensive and NaI detectors are well suited for the teaching of basic spectroscopic techniques where high resolution is not needed. High resolution gamma detectors are less common in the student laboratory but can significantly enhance the laboratory experience. The data are precise and plentiful, and high resolution detectors are ideal for analyzing environmental samples. For example, spectra from soil samples can have as many as 30 well-defined peaks, whose energy and area can be accurately measured. In this article, we present some of the experiments we perform in our senior-level nuclear radiation laboratory.

The experiments are designed to be “inquiry based” by having the students determine the best method to analyze the data themselves. Inquiry-based experiments have been shown to be effective in introductory laboratory classes,¹ and we find this approach also has value in our senior-level radiation laboratory. Initially, we do not give the students any guidelines for carrying out the analysis, although they have previous experience in the use of NaI detectors. In experiments with NaI gamma detectors, the students learn how to calibrate the detector for energy and photopeak efficiency; this knowledge is then applied to the high-resolution gamma detector.

The students can choose one of three types of samples, each one having a storyline to pique interest. One sample is a uranium-rich rock from the desert that is believed to be extra-terrestrial. It could also be from a rogue nation that is suspected of enriching uranium. The students’ task is to measure the natural abundance of ^{235}U in the rock and compare their value to 0.72%, the accepted value for natural samples from our planet. Another sample is a container of Brazil nuts that are suspected to be old. The students’ task is to determine the age of the nuts. A third option is a soil sample from the nearby area, usually soil from one of the students’ backyards. In this case, the students’ task is to identify the radioactive isotopes in the soil and measure their activity. In addition, the students are to determine if there is any contamination in their sample from nuclear fallout.

These experiments are a favorite among the students. They enjoy measuring a sample that they have collected, and they enjoy the independent nature of the activity in which they are not following a step-by-step method. They also are curious as to the amount of radiation in their backyards. For the soil and Brazil nut samples, data is collected for 20 h as

well as a 20-h spectrum without the sample present. We refer to the 20-h spectrum without a sample as the ambient background spectrum. During the week before the start of the experiment all the sample spectra are recorded. The whole experiment takes two three-hour laboratory sessions, during which each two-student group analyzes their own sample. In the sections that follow, we first discuss the detector calibration and data analysis and then describe each of the three experiments.

II. DATA ACQUISITION AND ANALYSIS

Our detector is a high-resolution, high-purity germanium (HPGe) detector,² which is connected to an 8196-channel MCA card. The HPGe detector has the advantage that it does not need to be continuously kept cool with liquid nitrogen while not in use. We cool our detector down three times during the school year for a two-to-three week period when we run the experiments for our radiation physics laboratory, radiation biology laboratory, and for special student projects. The detector sits atop a 30-l dewar; we order a 120-l container of LN₂ and fill/refill the detector dewar every four days. Data are acquired using the manufacturer’s software and then stored on the computer’s hard disk. All data analysis is done using software written by former students as special projects.³ Using Gaussian curve fitting techniques, the software allows the student user to extract the peak center, peak area, and the chi-square of the fit for the photopeaks. Five parameters are used to fit the photopeak: three for the Gaussian shape $he^{(x-E_\gamma)^2/(2\sigma^2)}$, and two for the background under the photopeak.³ The peak area corresponds to the total counts under the photopeak with this background subtracted.

The students begin their analyses by calibrating the HPGe detector following the same techniques they learned using the NaI detector. Using the calibration standards ^{137}Cs , ^{22}Na , ^{207}Bi , and ^{60}Co , the students determine the relationship between the energy of the gamma E_γ and channel number. For our setup, the relationship is remarkably linear, with the linearity being better than 0.01%. Another important relationship to determine is the width of the photopeak as a function of energy. Some photopeaks in the spectrum are produced by two gammas that are very close in energy. For these photopeaks, a single Gaussian shape will not produce a good fit and the width parameter σ will be larger than if the photopeak were produced by only a single gamma particle. To check if a photopeak is produced by only one gamma particle, the students plot the width parameter σ as a function of E_γ , as shown in Fig. 1. A common parameter for the resolution of a detector is the full width at half maximum (FWHM), which is related to σ by $\text{FWHM} = 2(\sqrt{2 \ln 2})\sigma$.

At an energy of 662 keV, the FWHM is around 1.3 keV, which is consistent with the manufacturer's specifications and other HPGe detectors.⁴ The relationship is approximately linear in E_γ with an offset.⁴ One can use the graph in Fig. 1 to check if a photopeak is the result of a single gamma. Once the detector is calibrated, the students continue their experiment by measuring the area under the photopeaks for the different gammas in the sample.

Most of the isotopes we use with our HPGe detector are from natural sources. The most abundant natural radioactive sources are ^{40}K and those from the ^{238}U , ^{235}U , and ^{232}Th decay series. In Tables I–III, we list the decay series data for ^{232}Th , ^{238}U , and ^{235}U . There are many gammas emitted in each series and we do not list them all; in the tables we list the radiation that is relevant for the environmental samples we measure (all data are obtained from Ref. 5). For each of the isotopes in the series, we list the energy of the gamma and the yield. The yield is the probability, in percent, that a gamma is emitted when the isotope decays. We note that there are some minor differences in the values of the yields listed in the references.⁵

The high-resolution spectra contain many gamma peaks from the daughter isotopes of the uranium and thorium decay series. Although it is easy to identify the energy of the gamma radiation, the students are generally at a loss as to how to proceed to determine the activity. From experience with our NaI detectors one expects a strong dependence of detector efficiency on gamma energy. At this point of the experiment, we carry out a classroom discussion on secular equilibrium, the importance of detector efficiency, and how to best handle the data. We start with the relationship between the counting rate C , the activity of the isotope A , the efficiency of the detector ϵ , and the gamma yield Y :

$$C = AY\epsilon. \quad (1)$$

The gamma yield Y depends on the isotope that emits the gamma and is the probability that a gamma of energy E_γ is emitted when the isotope decays. The yield values are listed in the last column in Tables I–III. We define the photo-peak efficiency ϵ as the number of gammas detected under the photo-peak divided by the number of gammas emitted for the particular detector-sample setup. The efficiency depends on the energy E_γ of the gamma, the detector-sample

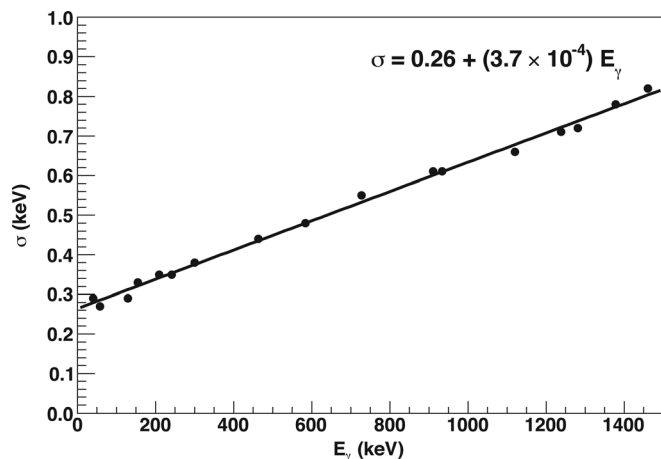


Fig. 1. A graph of the width parameter σ versus energy E_γ for our high-resolution gamma detector.

Table I. The ^{232}Th decay series.

Isotope	Half-life	E_γ (keV) (Yield)
^{232}Th	1.405×10^{10} years	63.8 (0.267%)
^{228}Ra	5.75 years	—
^{228}Ac	6.15 h	57.7 (0.487%)
		99.5 (1.28%)
		129.0 (2.42%)
		209.3 (3.88%)
		270.2 (3.43%)
		328.0 (2.95%)
		338.3 (11.3%)
		409.5 (1.94%)
		463.0 (4.44%)
		772 (1.50%)
		794.9 (4.36%)
		835.7 (1.61%)
		911.2 (26.6%)
		964.8 (5.11%)
		969.0 (16.2%)
^{228}Th	1.91 years	84.4 (1.22%)
^{224}Ra	3.64 days	241.0 (3.97%)
^{220}Rn	55 s	—
^{216}Po	0.15 s	—
^{212}Pb	10.64 h	238.6 (43.6%)
		300.0 (3.34%)
^{212}Bi	60.6 min	39.9 (1.1%)
		727.3 (6.65%)
64.06% ^{212}Po	304 ns	—
35.94% ^{208}Tl	3.1 min	277.4 (6.31%)
		510.77 (22.6%)
		583.2 (84.5%)
		763.1 (1.81%)
		860.6 (12.4%)
^{208}Pb	Stable	

geometry, and the absorption properties of the sample and detector. It is common to define efficiency as the probability that a particle is detected given that it enters the detector; that is, to break up ϵ into a factor dependent on the source-detector geometry and a factor dependent on the detector's counting ability. However, since the shape and position of the environmental sample and the KCl sample are the same, the detector-sample geometry is the same for all the gamma radiation in a particular experiment. For this reason we include the geometry factor in ϵ .

We then note that a useful quantity to consider is the counting rate divided by the yield C/Y . From the above equation this ratio equals $A\epsilon$. If a decay series is in secular equilibrium, then each daughter isotope has the same activity A . Thus, for the case of a decay series in secular equilibrium a plot of C/Y for the gammas emitted by the daughter isotopes versus their energy will result in a smooth curve, with the energy dependence proportional to the energy dependence of ϵ . A plot of C/Y versus energy is both a test to see if a decay series is in secular equilibrium and a portrayal of the energy dependence of ϵ . If the graph is not a smooth curve, then the sample is not in secular equilibrium.

After the discussion, it is apparent to the students that one needs to examine the counts-to-yield ratio C/Y using a sample that is known to be in secular equilibrium. For this

Table II. The ^{238}U decay series.

Isotope	Half-life	E_γ (keV) (Yield)
^{238}U	4.468×10^9 years	—
^{234}Th	24.1 days	63.3 (4.47%)
		92.38 (2.60%)
		92.80 (2.56%)
^{234}Pa	6.75 h	—
^{234}U	2.47×10^5 years	53.2 (0.123%)
^{230}Th	8.0×10^4 years	67.7 (0.373%)
^{226}Ra	1602 years	186.2 (3.59%)
^{222}Rn	3.823 days	—
^{218}Po	3.05 min	—
^{214}Pb	26.8 min	53.2 (1.1%)
		242.0 (7.46%)
		295.2 (19.2%)
		351.9 (37.1%)
		785.9 (1.09%)
		609.3 (46.1%)
		768.4 (4.89%)
		806.2 (1.23%)
		934.1 (3.16%)
		1120.3 (14.9%)
^{214}Bi	19.7 min	1238.1 (5.92%)
		1377.7 (4.02%)
		1408.0 (2.48%)
		1509.2 (2.19%)
		806.2 (1.23%)
^{214}Po	164 μs	—
^{210}Pb	21 years	46.5 (4.05%)
^{210}Bi	5.01 days	—
^{210}Po	138.4 days	—
^{206}Pb	Stable	—

purpose, we use an old lantern mantle that was purchased at a local hardware store.⁶ The older Coleman lantern mantles contain ^{232}Th . Gamma radiation from the isotopes ^{228}Ac , ^{228}Th , ^{224}Ra , ^{212}Pb , ^{212}Bi , and ^{208}Tl in the ^{232}Th series are plotted in Fig. 2. The isotope with the longest half-life in this group is ^{228}Th , which has a half-life of 1.91 years, and these six isotopes are in secular equilibrium. These older lantern mantles have enough activity for these isotopes to produce many clear peaks over a range of energy from 57.7–969 keV. Figure 2 shows a log-log plot of C/Y for these gamma peaks versus energy.

The graph in Fig. 2 is instructive. The smooth variation of C/Y indicates the ^{232}Th series is in secular equilibrium. Because the lantern mantle is a small sample, self-absorption is believed to be relatively small and the main energy dependence of C/Y is due to the efficiency of the detector. From the figure, it is seen that the detector has its maximum efficiency at around 90 keV. For higher energies, the efficiency decreases because the probability for photoabsorption decreases with energy. This is the second time the students have measured the photopeak efficiency as a function of gamma energy. In a previous experiment, the students measured the efficiency of their NaI gamma detector as a function of energy. Using calibrated standards ^{137}Cs , ^{22}Na , ^{60}Co , and ^{207}Bi , photopeak efficiencies for the NaI detector were obtained at gamma energies of 511, 570, 662, 1064, 1173, 1275, and 1332 keV. Using these calibrated standards we measured the absolute efficiency as a function of energy.

Table III. The ^{235}U decay series.

Isotope	Half-life	E_γ (keV) (Yield)
^{235}U	7.038×10^8 years	143.8 (10.96%)
		163.33 (5.08%)
		185.7 (57.2%)
		205.3 (5.01%)
^{231}Th	25.5 h	25.64 (14.5%)
		84.2 (6.6%)
^{231}Pa	3.28×10^4 years	27.4 (10.3%)
^{227}Ac	21.8 years	—
98.6% ^{227}Th	1.82 days	50.1 (8.0%)
		236.0 (12.3%)
		256.3 (7.0%)
		300 (2.3%)
		329.9 (2.7%)
1.4% ^{223}Fr	22 min	50.1 (36%)
		79.7 (9.1%)
^{223}Ra	11.43 days	234.8 (3%)
		144.2 (3.22%)
		154.2 (5.62%)
		269.5 (12.7%)
		323.9 (3.93%)
^{219}Rn	4 s	338.3 (2.79%)
		271.2 (10.8%)
		401.8 (6.37%)
^{215}Po	1.78 ms	—
^{211}Pb	36.1 min	404.9 (3.78%)
		427.1 (1.75%)
		832.0 (3.52%)
^{211}Bi	2.15 min	351.1 (12.95%)
^{207}Tl	4.79 min	—
^{207}Pb	Stable	—

In Fig. 2 the vertical axis is proportional to the efficiency of the detector; however, in both cases the shape of the curve, i.e., the energy dependence of the efficiency, is similar. The energy dependence in Fig. 2 agrees with the manufacturer's efficiency versus energy plot for the detector⁷ as well as published efficiency curves.^{8–10}

An important feature in Fig. 2 is the power-law dependence of C/Y versus energy for energies between 200 and

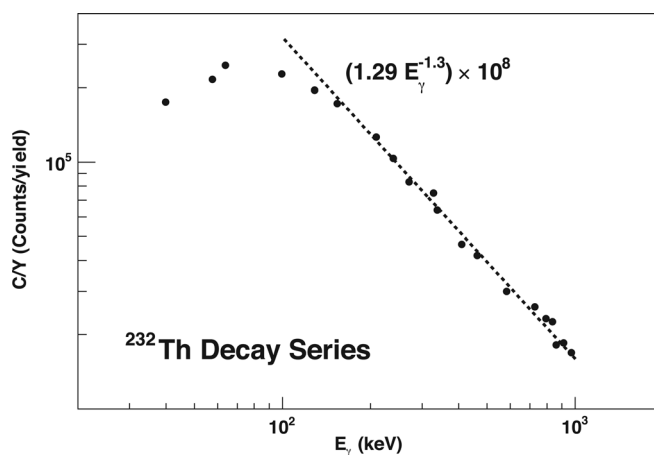


Fig. 2. A graph of the counts-to-yield ratio C/Y vs. energy E_γ for ^{232}Th using a lantern mantle as the sample. For gamma energies above 200 keV the data follows a power law, indicated by the dashed line.

1500 keV—a log-log plot of the function $\varepsilon(E)$ is approximately a straight line in this range. We demonstrate this property in Fig. 2 with the dashed line, which is a “best fit” power law function to the data within this range. We can use this empirical result to overcome the difficulty in comparing the area of gamma photopeaks at different energies, and hence to assist in determining the activity of the uranium and thorium decay series in our samples. We note that the slope of the best fit line for the log-log graph in the energy region 200–1500 keV will depend on the self-absorption of the sample. Because lower energy gammas are absorbed more readily, samples with less self-absorption will have a steeper slope. For our samples, the value of the slope generally lies between -1 and -1.3 (see Figs. 2–5, and 7) so self absorption is not a serious problem. Because nearly all the gammas that are measured have energies less than 1022 keV, escape of gammas due to pair creation is not significant. Even for the 1460 keV gamma from ^{40}K , which is used to calibrate the data, there are no observable escape peaks. We should mention that large volume HPGe detectors might not have a simple power law dependence for C/Y in the energy range 200–1500 keV, so a different energy range may be more appropriate for these detectors. It is, therefore, important to check C/Y for a sample known to be in secular equilibrium, as in Fig. 2, before analyzing other samples.

Next, we describe three experiments performed in our laboratory that make use of the C/Y plot to check if a sample is in secular equilibrium, determine isotope activities, and in one case, perform radioisotope dating of the sample.

III. SOIL SAMPLE EXPERIMENTS

For our soil sample experiments, the students are given the task of determining the activity of all isotopes in their soil. The samples we use are soil or rocks collected by students from around the area of our university. The soil is placed in a large plastic jar, which holds 3–4 kg of material, and is placed up against our detector.¹¹ The detector and sample are shielded with lead bricks. These experiments take on a special relevance for students because we let them bring in their own samples. Often they are surprised to discover that radioisotopes are present in their backyard.

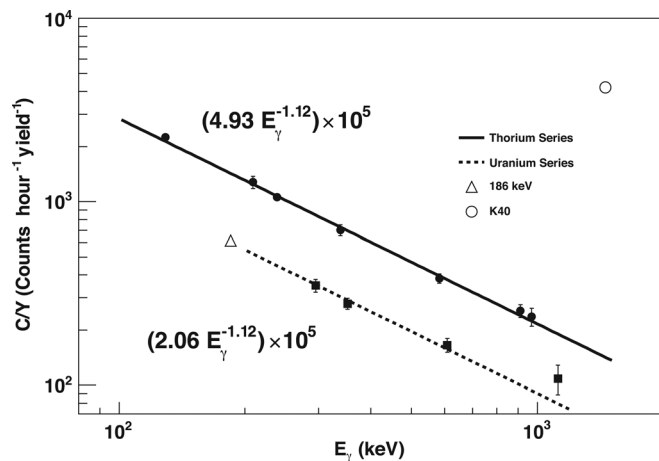


Fig. 3. A graph of C/Y vs. E_γ for a soil sample. The thorium series radiation is plotted with solid circles and the uranium series with solid squares. The C/Y value for the peak at 186 keV, which contains both ^{238}U and ^{235}U series gammas, is plotted as an open triangle. The 1460 keV ^{40}K radiation is plotted as an open circle.

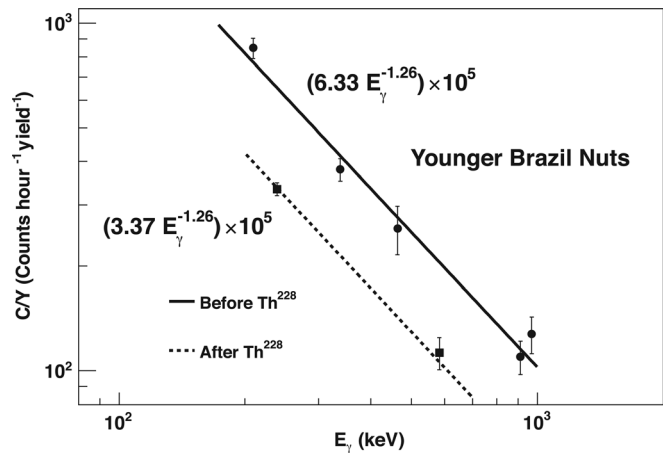


Fig. 4. A graph of C/Y vs. E_γ for “young” Brazil nuts. The radiation from ^{228}Ac , before ^{228}Th , is plotted as solid circles. The radiation from after ^{228}Th is plotted as solid squares.

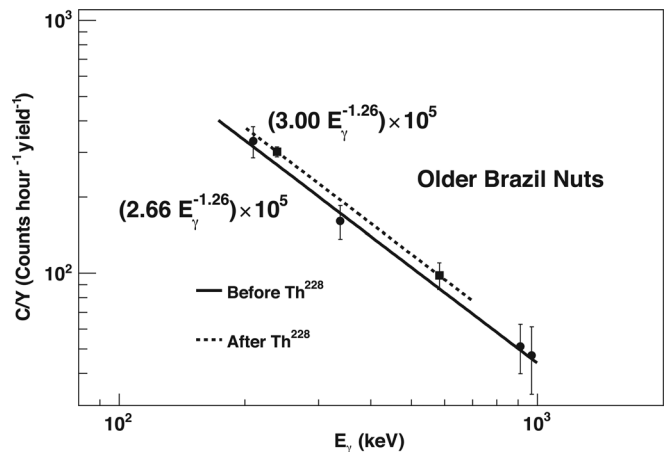


Fig. 5. A graph of C/Y vs. E_γ for “old” Brazil nuts. The radiation from ^{228}Ac , before ^{228}Th , is plotted as solid circles. The radiation from after ^{228}Th is plotted as solid squares.

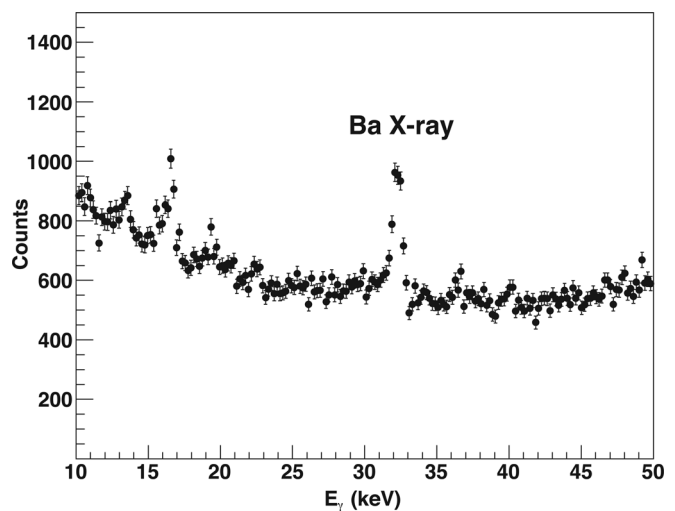


Fig. 6. A graph of counts vs. energy for the x-ray region of Brazil nuts. The photopeak at 32 keV is due to x-ray fluorescence of barium.

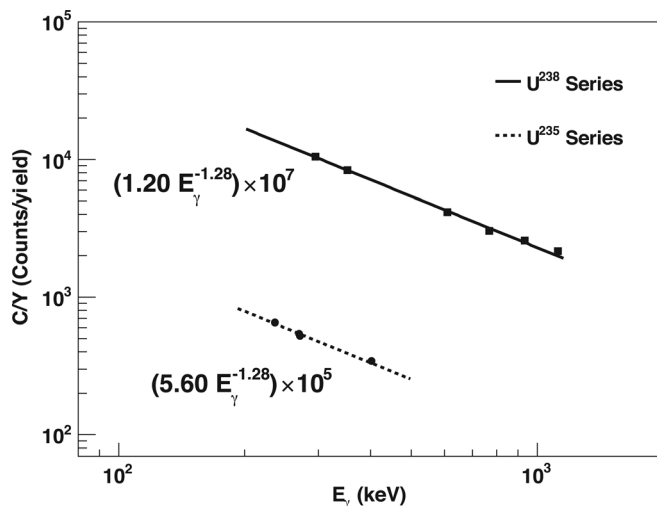


Fig. 7. A graph of C/Y vs. E_γ for the uranium series. The solid squares are for the ^{238}U series and the solid circles represent the ^{235}U series.

Three recordings are performed for the experiment: a 20-h ambient background with no sample present, a 20-h recording with the sample, and a 1-h recording of KCl having the same size, shape, and detector-source geometry as the sample. From these data, the students need to determine the amount of potassium in the soil in percent by weight, the activity of ^{238}U in units of Bq/kg, the activity of ^{232}Th in units of Bq/kg, and the amounts of any other radioactive isotopes present.

In Fig. 3, we plot C/Y versus energy for a local soil sample. It is important to determine the counts under the photopeak due to the sample itself, i.e., after subtracting the photopeak counts with no sample present. The data from both the ^{232}Th series and the ^{238}U series fall along smooth curves, consistent with each decay series being in secular equilibrium. The ^{238}U curve lies below the ^{232}Th curve implying that the activities from isotopes in the ^{238}U series are less than those of the ^{232}Th series.

A quantitative analysis can be carried out using suitable software. We have the students use the ROOT software from CERN to give them some experience with a data analysis program used in the nuclear and particle physics community. They enter their data into a sample program that minimizes a χ^2 function using TMinuit in the ROOT¹² package. The χ^2 function uses the same exponent for E_γ for both curves; that is, the three fitting parameters (a, b, c) for χ^2 are aE_γ^b for the ^{232}Th emissions and cE_γ^b for the ^{238}U gammas. The ratio a/c equals the ratio of the activities $\text{Act}(^{232}\text{Th series})/\text{Act}(^{238}\text{U series})$. The program outputs the fit parameters and a graph similar to that of Fig. 3.

One needs to be sure that no radon has escaped the sample when analyzing the gamma radiation from the isotopes of the ^{238}U decay series. All the measurable gamma radiation between 200 and 1500 keV from the ^{238}U decay series is emitted from isotopes that come after ^{222}Rn in the series. If the sample container is not completely air tight, some of the ^{222}Rn can escape. If this occurs the activity of the isotopes before ^{222}Rn will be larger than the activity of those after ^{222}Rn . We can check for any ^{222}Rn escape by measuring the counts under the photopeak at 186 keV. This photopeak is a double peak with one gamma, energy 186.2 keV, coming from ^{226}Ra , and another gamma, energy 185.7 keV, coming

from ^{235}U . Fortunately, ^{226}Ra is before ^{222}Rn in the ^{238}U decay series. If we assume that the natural abundance of ^{235}U in the soil is 0.72% and that the series $^{238}\text{U} \rightarrow ^{226}\text{Ra}$ is in secular equilibrium, then we can estimate the amount of radon lost from the sample. The relative yield of the 185.7 keV gamma equals 57.2% times the natural abundance of ^{235}U and the ratio of half-lives of the two uranium isotopes is $57.2(0.0072)(4.468 \times 10^9)/7.038 \times 10^8 = 57.2/21.88 = 2.61\%$. Thus, a factor of 21.88 reduces the yield of ^{235}U compared to ^{238}U . The large yield of the 185.7 keV gamma from ^{235}U has an effective yield of 2.61% and contributes significantly to the peak at 186 keV. Therefore, we can use a yield of $2.61 + 3.50 = 6.11\%$ for the 186 keV peak to plot C/Y for this peak. We can estimate the amount of radon that escaped by examining how this data point lines up with C/Y for the peaks of the ^{238}U series with energy greater than 200 keV. In Fig. 3, we plot C/Y for the 186 keV peak as an open triangle in the graph. Extending the C/Y points from the rest of the ^{238}U series, we see that the data are consistent with negligible radon escaping. Loss of radon can be reduced by making sure the container is air tight and waiting 20 days, more than five half-lives of ^{222}Rn , before taking data.

The 1460 keV gamma radiation from ^{40}K can be used to determine both the amount of potassium¹¹ and the absolute activity of the other radioisotopes present in the soil. To carry out the ^{40}K calibrations, data are recorded from a KCl sample that has the same shape and detector-source geometry as the bulk sample. The number of 1460 keV gammas emitted per second can be calculated from the mass of the KCl; our KCl sample has a mass of 3117 g. Knowing that the natural abundance of ^{40}K is 0.0117%, the number of ^{40}K nuclei in the sample is therefore $N_{40} = (3117/74.5)(6.02 \times 10^{23})(0.000117) \approx 2.94 \times 10^{21}$. The activity of ^{40}K in the KCl sample is $A = N \ln(2)/\tau = 2.94 \times 10^{21} \ln(2)/[1.29 \times 10^9(365)(24)] \approx 1.81 \times 10^8$ decays/hour, since the half-life of ^{40}K is 1.29×10^9 years. The number of 1460 keV gammas emitted per hour is $(1.81 \times 10^8)(0.1068) \approx 1.93 \times 10^7$, since the yield for the 1460 keV gamma is 0.1068. We recorded 6617 counts/hour for the sample, which gives an efficiency $\varepsilon(E = 1460 \text{ keV}) = 6617/(1.93 \times 10^7) \approx 3.42 \times 10^{-4}$ for the detector-source geometry of our sample.

The relative activity of the thorium series to that of the uranium series is found by simply taking the ratio of a to c . For the data shown in Fig. 3, we have $4.93/2.06 \approx 2.39$. To obtain the absolute activity, however, one needs a known standard for calibration. We use the KCl sample as our standard, which gives the efficiency at $E_\gamma = 1460 \text{ keV}$ for the detector-source geometry of our soil sample. The absolute activity in the soil is found by extrapolating the C/Y curve out to $E_\gamma = 1460 \text{ keV}$. The activity of the series is determined by dividing C/Y at 1460 keV by the efficiency at $E = 1460 \text{ keV}$. For example, C/Y for the ^{232}Th series in Fig. 3 equals $4.93E_\gamma^{-1.12} \times 10^5$ (counts/h)/yield. Equating this expression with $A\varepsilon$ gives $A(3.42 \times 10^{-4}) = 4.93(1460)^{-1.12} \times 10^5$. Solving for the activity A , one obtains 114 decays/sec for the ^{232}Th decay series in the soil. Since the soil has a mass of 4.66 kg, the specific activity is approximately 25 Bq/kg. The specific activity of the ^{238}U is then $25(2.06/4.93) \approx 10 \text{ Bq/kg}$. This method is fairly accurate because self-absorption for a 1460 gamma is small. For a more accurate estimate of $\varepsilon(E = 1460 \text{ keV})$, one can measure the area under the 1460 keV photopeak before and after a known amount of KCl is uniformly mixed into the soil.

Spiking a sample in this manner is a technique used to measure detector efficiency.¹⁰

Natural samples that are more radioactive than typical soil samples are also very interesting to investigate. We use a large rock sample that was donated to the university, and pitchblende also makes a good sample. In these more radioactive samples, emissions from the ^{235}U series can be detected and the ^{235}U natural abundance can be estimated. We discuss this possibility in Sec. V.

IV. BRAZIL NUTS EXPERIMENT

Brazil nuts are remarkable in that they grow in soil that is rich in thorium and uranium, and they have a strong affinity for radium. Consequently, the nuts contain a relatively large amount of radium from both the ^{238}U and the ^{232}Th decay series. ^{228}Ra from the ^{232}Th series is the most interesting to consider. ^{228}Ra has a half-life of 5.75 years. As shown in Table II, all the isotopes after ^{228}Ra have short half-lives except ^{228}Th , whose half-life is 1.91 years. Thus, one can use ^{228}Th as a “clock” to determine the “age” of the Brazil nut by examining C/Y before and after ^{228}Th . There is another thorium series radium isotope that is also brought up into the nut, ^{224}Ra . As it is brought up from the soil, it will have the same activity as ^{228}Ra , since the whole ^{232}Th series is in secular equilibrium in the soil. However, since its half-life is only 3.64 days compared to 1.91 years, the initial ^{224}Ra in the Brazil nut will decay away in a few weeks to the activity of the ^{228}Th initially in the nut.

As the Brazil nut grows in the tree, radium is brought up from the soil. Once in the nut, it starts to decay. It takes a Brazil nut around 14 months to mature in the tree before it falls to the ground. During this growing time the amounts of ^{228}Ra and the isotopes after ^{228}Ra in the series increase. After the nut falls from the tree, the ^{228}Ra is no longer replenished and it continues to decay along with the other isotopes in the series. After a few days the activity of ^{228}Ac will be the same as ^{228}Rn because the half-life of ^{228}Ac is only 6.13 h. After a few weeks, the activity of the isotopes following ^{228}Th will be the same as that of ^{228}Th . However, it will take around five half-lives of ^{228}Th , or ten years, for the whole series to come to transient equilibrium. During this time, we can “date” the nut by measuring C/Y for the emitted gammas.

As with the soil sample experiment, the students measure the counts under the photopeaks of the gamma radiation with the sample and subtract the corresponding counts with the sample removed. After the discussion on secular equilibrium, the students make a graph of the counts/yield ratio (C/Y) as a function of the energy of the gammas. In Figs. 4 and 5, we show two graphs of C/Y from Brazil nut samples, with the younger sample shown in Fig. 4. The gammas plotted are for energies with the highest yields. The five solid circles correspond to pre- ^{228}Th emissions of ^{228}Ac with energies (yields) of 209.3 keV (3.88%), 338.3 keV (11.3%), 463 keV (4.44%), 911 keV (26.6%), and 969 keV (16.2%). The two solid squares correspond to post- ^{228}Th emissions with energies (yields) of 238.6 keV (43.6%) and 583.2 keV ($0.845 \cdot 35.94 = 30.4\%$).

Figure 4 demonstrates that the decay series is not in secular equilibrium. The activity of ^{228}Ra , as measured from its daughter ^{228}Ac , which corresponds to the solid circles is

greater than the activity of ^{228}Th represented by the squares. The quantitative analysis of the data is performed by minimizing a χ^2 function using the root¹² TMinuit software from CERN, as described in Sec. III. As before, the χ^2 function uses the same exponent for E_γ for both curves; that is, the three fitting parameters (a, b, c) for χ^2 are aE_γ^b for the pre- ^{228}Th emissions and cE_γ^b for the post- ^{228}Th gammas. The ratio a/c equals the ratio of the activities $\text{Act}_C/\text{Act}_A$. We show in the Appendix that this ratio of activities for the Brazil nut series is given by

$$\frac{\text{Act}_C}{\text{Act}_A} \approx 1.50 - 1.30(1/2)^{t/2.86}, \quad (2)$$

where Act_C is the activity of the post- ^{228}Th isotopes and Act_A is the activity of the pre- ^{228}Th isotopes. By measuring the ratio of activities, the students can estimate the age of the nuts by solving for t in the equation above. In Fig. 4, we obtain $\text{Act}_C/\text{Act}_A \approx 3.37/6.33 \approx 0.53$, which gives a value of 1.2 years for the “age” of the nuts. In Fig. 5, the ratio $\text{Act}_C/\text{Act}_A$ is approximately 1.13, which gives 5.2 years for the Brazil nuts’ age. A nice feature of the analysis we use is that only the ratio of activities—not the absolute activities—is needed for dating the sample.

As an additional exercise, the students can also measure C/Y for the gammas given off in the ^{238}U series after ^{226}Ra . The isotope ^{226}Ra is also brought up from the soil into the Brazil nut and the isotopes that follow ^{226}Ra are in secular (or transient) equilibrium since the longest half-life is that of ^{222}Rn , 3.823 days. Here, the sample has to be airtight for at least three weeks to insure that no ^{222}Rn escapes the container. By comparing the C/Y graph of the ^{226}Ra series (from ^{238}U) with that of the ^{228}Ra series (from ^{232}Th), the students can estimate the relative amounts of uranium versus thorium in the soil where the Brazil nuts grew.

We mention one more interesting feature of the Brazil nut radiation. In Fig. 6, we plot the x-ray region of the Brazil nut spectrum. There is a photopeak at an energy near 32 keV, which corresponds to the characteristic x-ray of barium. The students have measured this x-ray in ^{137}Cs decay, however, there is no photopeak in the Brazil nut spectrum at 662 keV, which is the gamma energy given off when ^{137}Cs decays. The 32 keV emission comes from x-ray fluorescence of the barium in the nut. Brazil nuts contain a relatively large amount of barium that easily fluoresces when radiated. The radiation emitted from the two radium isotope series causes the barium in the nut to fluoresce.

We note that radioactive isotope dating using gamma spectra can be done with commercially produced samples. The age of a lantern mantle can be determined using a NaI detector once the efficiency as a function of gamma energy has been determined.⁹ Lantern mantles can also be dated using high-resolution gamma detectors by comparing the spectrum to that of a known amount of thorium ore, in secular equilibrium, with the same shape as the mantle.¹³ Since young lantern mantles are hard to find,⁶ one can also use welding rods.

V. ^{235}U ABUNDANCE EXPERIMENT

Another experiment that the students can choose is to estimate the natural abundance of ^{235}U in a sample that is rich in uranium. Because there is very little ^{235}U in nature, one needs a sample with a significant amount of uranium for the

^{235}U peaks to be accurately measured. For the abundance experiment, we use rocks donated to our department, samples from our Geology Department, or a sample of pitchblende that our department has purchased. The students are curious to test if the sample has been enriched or depleted. After the students have measured the counts under the many photopeaks present in the sample and our discussion of secular equilibrium, they make a plot of the counts/yield ratio C/Y for gammas emitted from the ^{238}U and ^{235}U decay series. As with the soil samples, one needs to be sure that no ^{222}Rn has escaped by keeping the sample sealed for a few weeks before measurements are taken.

In Fig. 7, we plot C/Y for isotopes in the ^{238}U decay series as well as the ^{235}U series from a uranium rich rock. The ^{235}U series data are plotted as solid circles and the ^{238}U series data are plotted as solid squares. The emissions from the ^{235}U series are much weaker than from the ^{238}U series. We find that the gamma emissions from the ^{235}U series that are the most consistent with the ^{238}U series have energies (yields) of: 236.0 keV (12.3%), 269.5 keV (12.7%), 271.2 keV (10.8%), and 401.8 keV (6.37%). These four peaks have the same energy dependence of C/Y as the ^{238}U series, as seen in Fig. 7. For the ^{238}U decay series in Fig. 7, we plot the gamma emissions with energy (yields) of: 295.2 keV (19.2%), 351.9 keV (37.1%), 609.3 keV (46.1%), 768.4 keV (4.89%), 934.1 keV (3.16%), and 1120 keV (14.9%).

The data are fit the same way as in the other experiments, by minimizing a χ^2 function using the ROOT¹² TMinuit software from CERN. As before, the χ^2 function uses the same exponent for E_γ for both curves. Here, we fit the ^{238}U series with aE_γ^b and the ^{235}U with cE_γ^b . The ratio c/a equals the ratio of the activities $\text{Act}(^{235}\text{U})/\text{Act}(^{238}\text{U})$. From Fig. 7, we see that the ratio c/a equals $(5.60 \times 10^5)/(1.20 \times 10^7) \approx 0.0467$. The natural abundance of ^{235}U is the ratio of the number of ^{235}U nuclei N_{235} to the number of ^{238}U nuclei N_{238} in the sample. The activity is related to the number of nuclei via the formula $\text{Act} = N \ln(2)/\tau$, where τ is the half-life. Thus, the natural abundance of ^{235}U is equal to $(c \tau_{235})/(a \tau_{238}) \approx 0.0467(7.09 \times 10^8)/(4.47 \times 10^9) \approx 0.0074$, or $(0.74 \pm 0.03)\%$. The percent errors in c and a from the chi-square fit¹² are both 1.9%, giving a 3.8% uncertainty, or ± 0.03 , in the natural abundance. The accepted value for the ^{235}U natural abundance is 0.72%. As in the case of radioisotope dating, only the ratio of activities is needed and not the absolute activities.

VI. SUMMARY

We have described experiments using environmental samples that one can perform in an undergraduate nuclear physics laboratory with a high-resolution gamma detector. The key quantity to consider is the counts (C) under a photopeak divided by the yield (Y) of the radiation. By plotting C/Y versus the energy of the gamma, one can examine if the sample is in secular equilibrium, determine the relative amounts of isotopes in the sample, and for the case of Brazil nuts, perform radioisotope dating.

ACKNOWLEDGMENTS

The authors would like to thank the many students in our senior level radiation laboratory class who collected and

analyzed the environmental samples during the past 12 years. A special thanks goes to Cal Poly Pomona physics majors Linda Ostos, Mark McGovern, Tsuyoshi Kawahito (TK), Susan Hoppe, Matt Smith, Andres Cardenas, Phu Tran, Josh Zeeman, and Mike Hatfield for their assistance in this project.

APPENDIX: RATIO OF ACTIVITIES FOR BRAZIL NUTS

The dynamics of the radioisotope decay chain are described by the Bateman equations.¹⁴ Different solutions to the Bateman equations have been described in this journal,^{15–18} as have experiments to observe the transition to secular equilibrium.¹⁹ We need to apply the Bateman equations to the uptake and subsequent decay of radium in Brazil nuts. There are two stages to consider: (1) the period when the Brazil nut is growing in the tree, and (2) the period after the Brazil nut has fallen to the ground. In both cases there are essentially two half-lives that enter the calculation, the half-life of ^{228}Ra and that of ^{228}Th . This is because these two isotopes have significantly longer half-lives than the other isotopes in the decay series. The half-life of ^{228}Ra is 5.75 years, the half-life of ^{228}Th is 1.91 years, and the next longest half-life is only 3.64 days, for ^{224}Ra . Consequently there are essentially only two relevant activities. One activity is that of ^{228}Ra and ^{228}Ac , which are equal. The other activity is that of ^{228}Th and all its daughters, which also have the same activity as ^{228}Th after a few weeks.

A. First stage: Brazil nut growing

Consider the first stage when the Brazil nut is growing in the tree. Let $N_A(t)$ be the number of ^{228}Ra nuclei in the nut at time t . Then N_A satisfies the differential equation

$$\frac{dN_A}{dt} = \alpha - N_A \lambda_A, \quad (\text{A1})$$

where α is the rate at which ^{228}Ra is brought up into the nut and λ_A is the decay constant for ^{228}Ra . The solution to this equation is

$$N_A = \frac{\alpha}{\lambda_A} (1 - e^{-\lambda_A t}), \quad (\text{A2})$$

for the initial condition $N_A(0) = 0$. Because the activity of ^{228}Ra is equal to $\lambda_A N_A$, we have

$$\text{Act}(^{228}\text{Ra}) = \alpha (1 - e^{-\lambda_A t}) \quad (\text{A3})$$

for the activity of ^{228}Ra in the Brazil nut after a growing period of time t .

Using Eq. (A3), we can determine the activity of ^{228}Th in the Brazil nut during its growth. Let N_B be the number of ^{228}Th nuclei in the nut at time t while the nut is growing. This number satisfies the differential equation

$$\frac{dN_B}{dt} = \lambda_A N_A - N_B \lambda_B, \quad (\text{A4})$$

where λ_B is the decay constant for ^{228}Th . The quantity $\lambda_A N_A$ is the activity of ^{228}Ra , which is the rate at which ^{232}Th is produced. We use the activity of ^{228}Ra in this expression because both ^{228}Ac and ^{228}Ra have essentially the same activity due to the short half-life of ^{228}Ac compared to ^{228}Ra .

Solving Eq. (A4) gives

$$N_B = \alpha \left(\frac{\lambda_A}{\lambda_B(\lambda_B - \lambda_A)} e^{-\lambda_B t} + \frac{e^{-\lambda_A t}}{\lambda_A - \lambda_B} + \frac{1}{\lambda_B} \right) \quad (\text{A5})$$

for the initial condition $N_B(0) = 0$. As before, the activity of ^{228}Th is given by $\lambda_B N_B$ so we have

$$\text{Act}(^{228}\text{Th}) = \alpha \left(\frac{\lambda_A}{\lambda_B - \lambda_A} e^{-\lambda_B t} + \frac{\lambda_B e^{-\lambda_A t}}{\lambda_A - \lambda_B} + 1 \right) \quad (\text{A6})$$

for the activity of ^{228}Th in the Brazil nut after a growing time t .

The main factor in determining the age of the Brazil nut is the ratio of the activities of ^{228}Th to that of ^{228}Ra : $\text{Act}(^{228}\text{Th})/\text{Act}(^{228}\text{Ra})$. We will need to know what this ratio is when the nut falls from the tree. For a growing time of $t = 14$ months and $\lambda_A = \ln(2)/5.75 \text{ years}^{-1}$, we have $\text{Act}(^{228}\text{Ra}) \approx 0.131\alpha$ from Eq. (A3). Using these parameters and $\lambda_B = \ln(2)/1.91 \text{ years}^{-1}$ gives $\text{Act}(^{228}\text{Th}) \approx 0.026\alpha$ from Eq. (A6). The ratio of the ^{228}Th to the ^{228}Ra activity is therefore

$$\frac{\text{Act}(^{228}\text{Th})}{\text{Act}(^{228}\text{Ra})} \approx \frac{0.026\alpha}{0.131\alpha} \approx 0.20 \quad (\text{A7})$$

when the nut falls from the tree. Note that the rate of uptake α cancels out in this ratio.

B. Second stage: After falling from the tree

Now consider the time after the nut has fallen from the tree. The number of ^{228}Ra nuclei in the nut, N'_A , satisfies the differential equation

$$\frac{dN'_A}{dt} = -N'_A \lambda_A, \quad (\text{A8})$$

which is the same as before but without the growth term α . The solution for times t after the nut falls from the tree is

$$N'_A(t) = N'_0 e^{-\lambda_A t}, \quad (\text{A9})$$

where N'_0 represents the number of ^{228}Ra nuclei just after the nut falls from the tree.

As in the initial stage, the number of ^{228}Th nuclei N'_B satisfies the differential equation

$$\frac{dN'_B}{dt} = \lambda_A N'_A - N'_B \lambda_B. \quad (\text{A10})$$

After substituting $N'_A e^{-\lambda_A t}$ for N'_A and solving the differential equation, one obtains¹⁸

$$N'_B(t) = \frac{\lambda_A N'_0}{\lambda_B - \lambda_A} (e^{-\lambda_A t} - e^{-\lambda_B t}) + N'_B(0) e^{-\lambda_B t}. \quad (\text{A11})$$

Here $N'_B(0)$ is the initial number of ^{228}Th nuclei. To compare with experiment one needs to calculate the ratio of the activities of ^{228}Th , given by $\lambda_B N'_B(t)$, to ^{228}Ra , given by $\lambda_A N'_A(t) = N'_0 e^{-\lambda_A t}$. Using the equations above we obtain

$$\frac{\text{Act}(^{228}\text{Th})}{\text{Act}(^{228}\text{Ra})} = \frac{\lambda_B}{\lambda_B - \lambda_A} (1 - e^{(\lambda_A - \lambda_B)t}) + 0.20 e^{(\lambda_A - \lambda_B)t}, \quad (\text{A12})$$

since the initial ratio of $\text{Act}(^{228}\text{Th})/\text{Act}(^{228}\text{Ra})$ is approximately 0.20. Using the decay constants $\lambda_A = \ln(2)/5.75 \text{ years}^{-1}$ and $\lambda_B = \ln(2)/1.91 \text{ years}^{-1}$, we obtain an expression that can be compared with the data:

$$\frac{\text{Act}(^{228}\text{Th})}{\text{Act}(^{228}\text{Ra})} \approx 1.50 - 1.30(1/2)^{t/2.86}, \quad (\text{A13})$$

where t is in years and we have changed from base e to base 2. Note that the ratio of activities varies from 0.20 to 1.5 with an effective “half life” of 2.86 years.

^{a)}Electronic mail: pbsiegel@csupomona.edu

¹L. C. McDermott and E. F. Redish, “Resource letter PER-1: Physics education research,” *Am. J. Phys.* **67**(9), 755–768 (1999).

²We use a high resolution germanium gamma detector from Canberra, model number BE2020. The detector interfaces to a PC with an 8192 channel MCA card from Canberra. The data is saved as a *.cnf file and analyzed with student-written software.

³Byron Curry, Dave Riggins, and P. B. Siegel, “Data analysis in the undergraduate nuclear laboratory,” *Am. J. Phys.* **63**, 71–76 (1995).

⁴K. Szymanska *et al.*, “Resolution, efficiency and stability of HPGe detector operating in a magnetic field at various gamma-ray energies,” *Nucl. Instrum. Methods Phys. Res. A* **592**, 486–492 (2008).

⁵The data for the decay series were obtained from the web sites <atom.kaeri.re.kr> and <t2.lanl.gov.data/map.html>.

⁶T. Toepker, “Thorium and yttrium in gas lantern mantles,” *Am. J. Phys.* **64**(2), 109 (1996). This letter points out that newer Coleman lantern mantles don’t contain thorium.

⁷Canberra Broad Energy Germanium Detectors data sheet, <<http://www.canberra.com/products/detectors/pdf/BEGe-SS-C40013.pdf>>.

⁸G. F. Knoll, *Radiation Detection and Measurement* (Wiley, New York, 1979). See Figs. 12–24a and 12–25a for a plot of efficiency vs. energy.

⁹R. S. Peterson, *Experimental γ Ray Spectroscopy and Investigations of Environmental Radioactivity* (Spectrum Techniques, Oak Ridge, TN, 1996).

¹⁰I. Vukanac *et al.*, “Experimental determination of the HPGe spectrometer efficiency curve,” *Appl. Radiat. Isot.* **66**, 792–795 (2008). In this article soil (Fig. 1) and water (Fig. 1) samples were spiked with radioactive isotopes to determine the detector’s photopeak efficiency curve.

¹¹Barbara Hoeling, Douglas Reed, and P. B. Siegel, “Going bananas in the radiation laboratory,” *Am. J. Phys.* **67**, 440–442 (1999). See Fig. 1 for a diagram of our setup.

¹²We use the TMinuit class in the root software from CERN to do the chi-square minimization. We use this package to give students experience with the ROOT software, however other software can be used.

¹³J. Luetzelschwab, “Determining the age of gas lantern mantles using gammaray analysis,” *Am. J. Phys.* **51**(6), 538–542 (1983).

¹⁴H. Bateman, “The solution of a system of differential equations occurring in the theory of radioactive transformations,” *Proc. Cambridge Philos. Soc.* **15**, 423–427 (1910).

¹⁵D. S. Pressyanov, “Short solution of the radioactive decay chain equations,” *Am. J. Phys.* **70**, 444–445 (2002).

¹⁶L. Moral and A. F. Pacheco, “Algebraic approach to the radioactive decay equations,” *Am. J. Phys.* **71**, 684–686 (2003).

¹⁷Ding Yuan, “Linear transformation method for multinuclide decay calculation,” *Am. J. Phys.* **78**, 1346–1351 (2010).

¹⁸M. L. Boas, *Mathematical Methods in the Physical Sciences*, 3rd ed. (John Wiley & Sons, New York, 2006), pp. 402–403.

¹⁹C. T. Angell, A. C. Kaplan, J. D. Seelig, E. B. Norman, and M. Pedretti, “Concepts in nuclear science illustrated by experiments with radon,” *Am. J. Phys.* **80**, 61–65 (2012).